The University of Nottingham

UNITED KINGDOM · CHINA · MALAYSIA

Padmanaban, Sanjeevikumar and Hontz, Michael R. and Khanna, Raghav and Wheeler, Patrick William and Blaabjerg, Frede and Ojo Olorunfemi, Joseph (2016) Isolated/non-isolated quad-inverter configuration for multilevel symmetrical/asymmetrical dual six-phase star-winding converter. In: 2016 IEEE 25th International Symposium on Industrial Electronics (ISIE), 8-10 June 2016, St Clara, California, USA.

Isolated/Non-Isolated Quad-Inverter Configuration For Multilevel Symmetrical/Asymmetrical Dual Six-Phase Star-Winding Converter

Sanjeevikumar Padmanaban
Research and Development,
Power Electronics Division,
Ohm Technologies, Chennai, India.
sanjeevi_12@yahoo.co.in

Michael R. Hontz
Electrical Engineering & Computer Science Dept., University of Toledo,
Toledo, Ohio, USA.
michael.hontz@rockets.utoledo.edu

Raghav Khanna
Electrical Engineering & Computer Science Dept., University of Toledo,
Toledo, Ohio, USA.
raghav.khanna@utoledo.edu

Patrick William Wheeler
Power Electronics, Machines and Control Group (PEMC), Dept. of Electrical & Electronics Engg.,
Nottingham University, UK.
pat.wheeler@nottingham.ac.uk

Frede Blaabjerg
Center for Reliable Power Electronics, (CORPE), Dept. of Energy Technology,
Aalborg University, Denmark.
fbl@et.aau.dk

Joseph Olorunfemi Ojo
Dept. of Electrical & Computer Engg., Tennessee Technological University, USA. University of KwaZulu-Natal, Durban, South Africa.
jojo@tntech.edu

***Abstract*—This article presents the developments of a novel isolated/non-isolated quad inverter configuration for multilevel dual six-phase (twelve-phase) star-winding converter. The modular circuit consists of four standard voltage source inverters (VSIs). Each VSI is incorporated with one bi-directional switch (MOSFET/IGBT) per phase and links with the neutral line through two capacitors which allows symmetrical and asymmetrical operations. A modified single carrier five-level modulation (MSCFM) algorithm is developed and modulates each 2-level VSI as a 5-level output multilevel inverter. The entire AC converter is numerically modeled using Matlab/PLECS simulation software and the predicted behavior of the system is analyzed and presented. Good agreement is obtained between these results and the theoretical analysis. Suitable applications for the converter include (low-voltage/high-current) medium power systems, electrical vehicles, AC tractions, and 'More-Electric Aircraft' propulsion systems.**

Keywords—Dual six-phase inverter, twelve-phase inverter, multilevel inverters, motor drives, multiple space vectors, split-phase space vector transformation, pulse-width modulation.

I. INTRODUCTION

Multiphase AC drives are well-regarded due to their high reliability, redundant structure, limited DC link ripple, increased power density, fault tolerance, and reduced per-phase inverter rating (low-voltage/high-current) [1-7]. This article develops an isolated/non-isolated twelve-phase multilevel converter derived from quad-inverter configuration for star-winding loads. The twelve phases are achieved by two adjacent windings which are spatially phase shifted by 30^0 (symmetrical type) [2-6] or by 15^0 (asymmetrical) [2, 7]. The novelty of the converter is that it demonstrates the feasibility of splitting the windings into standard three-phase groups as shown in Fig. 1 which are then driven by multiple classical voltage source inverters [2, 3-7]. Such topologies can be configured and are termed dual-, triple-, or quadruple multiphase-phase AC drives [2-7]. Recently, these systems have found applications in 'More-Electric Aircraft' (MEA) [8-9], where they are applied as the alternatives to hydraulic and pneumatic actuators. In this application, reliability in fault conditions is guaranteed and overall aeronautic propulsion is improved in MEA [9].

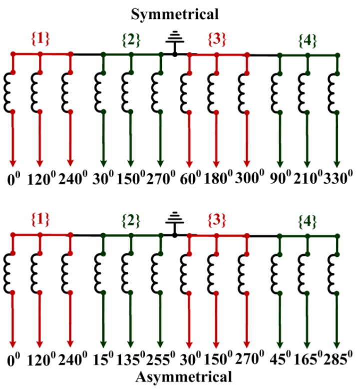

Fig. 1. Split-phases of twelve-phase windings as standard three-phase windings as groups.

Multilevel inverters (MLIs) are a viable solution to a high voltage synthesis by sources and devices of limited rating while also providing reduced total harmonic distortion (THD), and dv/dt in the output voltages [10-11]. It has been shown, that the multi-phase and multi-level inverter combined configuration is a sufficient solution for redundancy and fault tolerance in drives [1-7]. Still potential failures persist in multilevel inverters, chiefly in the power parts (31-37.9%) due to the limitations of IGBT devices for high-power applications, discrete capacitors and current gate control techniques [11-12]. The reliability of the standard 2-level VSI is still a factor in a multi-phase and multi-level inverter configuration as this system utilizes multiple VSIs arrangements [2, 4-7]. In topologies referred to as dual inverters, the two multiphase VSIs (two-level) are incorporated at each end of the open-windings [2-6]. Each leg's potential difference between two single VSIs constitutes the 3-level outputs when subjected to each pair of VSIs as a 3-level PWM modulation signal. Multiphase dual inverters offer greater benefits in comparison to standard MLIs [2, 4-6] and common-mode components can be minimized by the PWM strategies or by employing isolated

978-1-5090-0872-8/16/$31.00

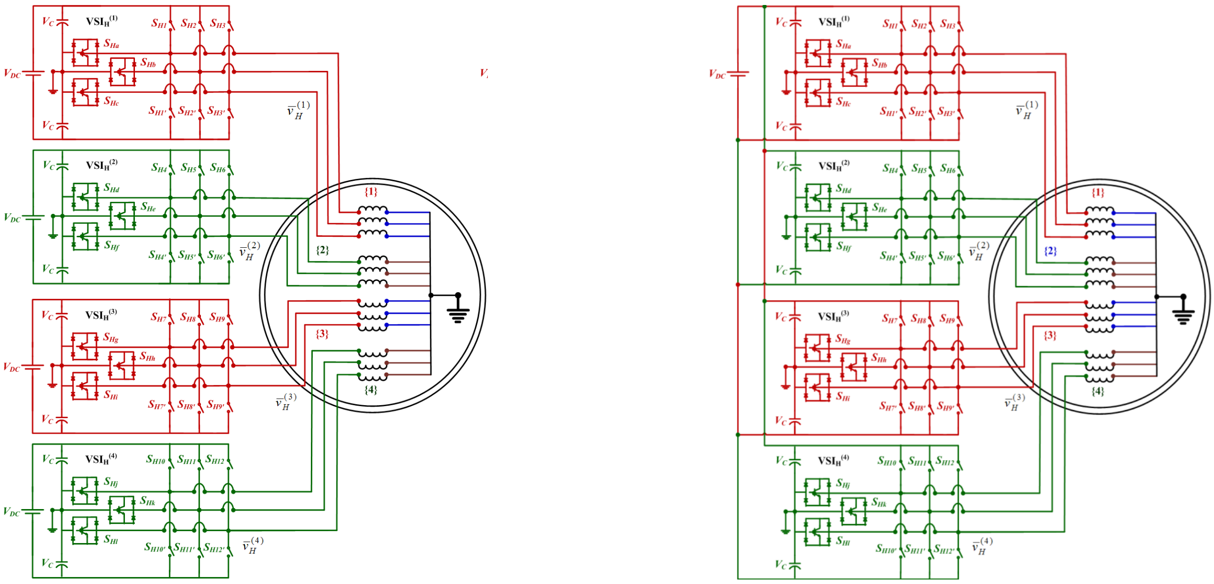

Fig. 2. Proposed configuration of quad-inverter system for asymmetrical/symmetrical dual six-phase star-winding multilevel converter. **Left:** isolated version, **Right:** Non-isolated version.

This paper deals primarily with a novel configuration for a dual six-phase (double quad or twelve-phase) isolated/non-isolated multilevel star-winding converter as shown in Fig. 2 [2, 4-7]. A modified single carrier five-level modulation (MSCFM) algorithm is developed and ensures 5-level modulated VSIs outputs [15-16]. The modular structure consists of four classical two-level, three-phase VSIs with one bi-directional (IGBT) switch incorporated per phase which are linked to neutral through two capacitors. Each VSI is connected across three-phase star-windings $VSI_H^{(1)}$ {1}, $VSI_H^{(2)}$ {2}, $VSI_H^{(3)}$ {3}, and $VSI_H^{(4)}$ {4} to ensure 5-levels in each leg's phase [13]. The total power is split amongst the four DC sources (asymmetrical) and allows quadrupling of the power capabilities of each VSI. Redundancy allows for the failure of up to three VSIs, while maintaining operation with one VSI. Under this fault condition despite the system remains operable, the output power is reduced. Furthermore, the novel configuration combines the benefits of standard MLIs, with scalability to more than 12-phases in multiples of 3 with a redundant structure that is fault tolerant [2, 4-7].

To verify its performance, the proposed isolated/ non-isolated twelve-phase symmetrical/asymmetrical AC converter is numerically modelled with Matlab/PLEC simulation software. Tests are conducted with balanced conditions for both the symmetrical and asymmetrical converter configurations. The observed results are presented in this paper and show good agreement with the theoretical analysis.

II. SPLIT-PHASE DECOMPOSITION SPACE VECTOR TRANSFORMATION

The dual six-phase star-winding system can be represented by stationary multiple space vectors as [2, 4-6]:

$$
\begin{aligned}
\bar{x}_1 &= \frac{1}{4}\begin{bmatrix} x_1 + x_2\alpha^4 + x_3\alpha^8 + x_4\alpha + \\ x_5\alpha^5 + x_6\alpha^9 + x_7\alpha^2 + x_8\alpha^6 + \\ x_9\alpha^{10} + x_{10}\alpha^3 + x_{11}\alpha^7 + x_{12}\alpha^{11} \end{bmatrix} \\
\bar{x}_3 &= \frac{1}{4}\left[\begin{pmatrix} x_1 + x_2 + x_3 + \\ x_4 + x_5 + x_6 \end{pmatrix} + j\begin{pmatrix} x_7 + x_8 + x_9 + \\ x_{10} + x_{11} + x_{12} \end{pmatrix}\right] \\
\bar{x}_5 &= \frac{1}{4}\begin{bmatrix} x_1 + x_2\alpha^8 + x_3\alpha^4 + x_4\alpha^5 + \\ x_5\alpha^9 + x_6\alpha^{13} + x_7\alpha^{10} + x_8\alpha^{14} + \\ x_9\alpha^{18} + x_{10}\alpha^{15} + x_{11}\alpha^{19} + x_{12}\alpha^{23} \end{bmatrix} \\
\bar{x}_7 &= \frac{1}{4}\begin{bmatrix} x_1 + x_2\alpha^4 + x_3\alpha^8 + x_4\alpha^7 + \\ x_5\alpha^{11} + x_6\alpha^{15} + x_7\alpha^{14} + x_8\alpha^{18} + \\ x_9\alpha^{22} + x_{10}\alpha^{21} + x_{11}\alpha^{25} + x_{12}\alpha^{29} \end{bmatrix} \\
\bar{x}_9 &= \frac{1}{4}\left[\begin{pmatrix} x_7 + x_8 + x_9 + \\ x_{10} + x_{11} + x_{12} \end{pmatrix} + j\begin{pmatrix} x_1 + x_2 + x_3 + \\ x_4 + x_5 + x_6 \end{pmatrix}\right] \\
\bar{x}_{11} &= \frac{1}{4}\begin{bmatrix} x_1 + x_2\alpha^8 + x_3\alpha^4 + x_4\alpha^{11} + \\ x_5\alpha^{15} + x_6\alpha^{19} + x_7\alpha^{22} + x_8\alpha^{26} + \\ x_9\alpha^{30} + x_{10}\alpha^{33} + x_{11}\alpha^{37} + x_{12}\alpha^{41} \end{bmatrix}
\end{aligned}
\qquad (1)
$$

$$
\bar{x}_1 = \frac{1}{4}\begin{bmatrix} x_1 + x_2\alpha^8 + x_3\alpha^{16} + x_4\alpha + \\ x_5\alpha^9 + x_6\alpha^{17} + x_7\alpha^2 + x_8\alpha^{10} + \\ x_9\alpha^{18} + x_{10}\alpha^3 + x_{11}\alpha^{11} + x_{12}\alpha^{19} \end{bmatrix} \qquad (2)
$$

$$\overline{x}_3 = \frac{1}{4}\left[\begin{pmatrix} x_1 + x_2 + x_3 + \\ x_4 + x_5 + x_6 \end{pmatrix} + j\begin{pmatrix} x_7 + x_8 + x_9 + \\ x_{10} + x_{11} + x_{12} \end{pmatrix}\right]$$

$$\overline{x}_5 = \frac{1}{4}\begin{bmatrix} x_1 + x_2\alpha^{16} + x_3\alpha^8 + x_4\alpha^5 + \\ x_5\alpha^{21} + x_6\alpha^{13} + x_7\alpha^{10} + x_8\alpha^{26} + \\ x_9\alpha^{18} + x_{10}\alpha^{15} + x_{11}\alpha^{31} + x_{12}\alpha^{23} \end{bmatrix}$$

$$\overline{x}_7 = \frac{1}{4}\begin{bmatrix} x_1 + x_2\alpha^{8} + x_3\alpha^{16} + x_4\alpha^7 + \\ x_5\alpha^{15} + x_6\alpha^{23} + x_7\alpha^{14} + x_8\alpha^{22} + \\ x_9\alpha^{30} + x_{10}\alpha^{21} + x_{11}\alpha^{29} + x_{12}\alpha^{37} \end{bmatrix}$$

$$\overline{x}_9 = \frac{1}{4}\left[\begin{pmatrix} x_7 + x_8 + x_9 + \\ x_{10} + x_{11} + x_{12} \end{pmatrix} + j\begin{pmatrix} x_1 + x_2 + x_3 + \\ x_4 + x_5 + x_6 \end{pmatrix}\right]$$

$$\overline{x}_{11} = \frac{1}{4}\begin{bmatrix} x_1 + x_2\alpha^{16} + x_3\alpha^8 + x_4\alpha^{11} + \\ x_5\alpha^{27} + x_6\alpha^{19} + x_7\alpha^{22} + x_8\alpha^{38} + \\ x_9\alpha^{30} + x_{10}\alpha^{33} + x_{11}\alpha^{49} + x_{12}\alpha^{41} \end{bmatrix}$$

where, $\alpha = exp\ (j2\pi/12)$ for the symmetrical converter in (1), and $\alpha = exp\ (j\pi/12)$ for the asymmetrical converter version, as the displacement between windings [3, 7].

The multiple space vectors $\overline{x}_1, \overline{x}_5, \overline{x}_7, \overline{x}_{11}$ are rotating vectors and $\overline{x}_3, \overline{x}_9$ are the common-mode components available in sub-spaces of d_1-q_1, d_5-q_5, d_7-q_7, d_{11}-q_{11} and d_3-q_3, d_9-q_9 respectively.

The split-phase space vector decomposition transformation was applied to the dual six-phase star-windings supplied by four VSIs with isolated or non-isolated DC sources. The system can be split into four three-phase sub-systems {1}, {2}, {3}, {4} and investigated as such [2, 7]:

$$\{1\}\begin{cases} x_1^{(1)} = x_1 \\ x_2^{(1)} = x_2 \\ x_3^{(1)} = x_3 \end{cases};\ \{2\}\begin{cases} x_1^{(2)} = x_4 \\ x_2^{(2)} = x_5 \\ x_3^{(2)} = x_6 \end{cases};\ \{3\}\begin{cases} x_1^{(3)} = x_7 \\ x_2^{(3)} = x_8 \\ x_3^{(3)} = x_9 \end{cases};\ \{4\}\begin{cases} x_1^{(4)} = x_{10} \\ x_2^{(4)} = x_{11} \\ x_3^{(4)} = x_{12} \end{cases}. \quad (3)$$

The multiple space vectors, $\overline{x}^{(2)}$, $\overline{x}^{(3)}$, and $\overline{x}^{(4)}$ as well as the homo-polar components $x_0^{(1)}$, $x_0^{(2)}$, $x_0^{(3)}$, $x_0^{(4)}$ are stated for four three-phase sub-systems {1}, {2}, {3} and {4} as below:

$$\{1\}\begin{cases} \overline{x}^{(1)} = \frac{2}{3}\left[x_1^{(1)} + x_2^{(1)}\alpha^4 + x_3^{(1)}\alpha^8\right] \\ x_0^{(1)} = \frac{1}{3}\left[x_1^{(1)} + x_2^{(1)} + x_3^{(1)}\right] \end{cases}$$

$$\{2\}\begin{cases} \overline{x}^{(2)} = \frac{2}{3}\left[x_1^{(2)} + x_2^{(2)}\alpha^4 + x_3^{(2)}\alpha^8\right] \\ x_0^{(2)} = \frac{1}{3}\left[x_1^{(2)} + x_2^{(2)} + x_3^{(2)}\right] \end{cases}$$

$$\{3\}\begin{cases} \overline{x}^{(3)} = \frac{2}{3}\left[x_1^{(3)} + x_2^{(3)}\alpha^4 + x_3^{(3)}\alpha^8\right] \\ x_0^{(3)} = \frac{1}{3}\left[x_1^{(3)} + x_2^{(3)} + x_3^{(3)}\right] \end{cases} \quad (4)$$

$$\{4\}\begin{cases} \overline{x}^{(4)} = \frac{2}{3}\left[x_1^{(4)} + x_2^{(4)}\alpha^4 + x_3^{(4)}\alpha^8\right] \\ x_0^{(4)} = \frac{1}{3}\left[x_1^{(4)} + x_2^{(4)} + x_3^{(4)}\right] \end{cases}$$

Multiple space vectors and split-phase space vectors are related by substituting (4) and (3) into (1) and (2), summarized below:

$$\begin{aligned}
\overline{x}_1 &= \frac{1}{4}\left[\overline{x}^{(1)} + \alpha\,\overline{x}^{(2)} + \alpha^2\overline{x}^{(3)} + \alpha^3\,\overline{x}^{(4)}\right] \\
\overline{x}_5^* &= \frac{1}{4}\left[\overline{x}^{(1)} + \alpha^5\,\overline{x}^{(2)} + \alpha^{10}\overline{x}^{(3)} + \alpha^{15}\,\overline{x}^{(4)}\right] \\
\overline{x}_3 &= x_0^{(1)} + x_0^{(2)} + j(x_0^{(3)} + x_0^{(4)}) \\
\overline{x}_7 &= \frac{1}{4}\left[\overline{x}^{(1)} + \alpha^7\,\overline{x}^{(2)} + \alpha^{14}\overline{x}^{(3)} + \alpha^{21}\,\overline{x}^{(4)}\right] \\
\overline{x}_{11}^* &= \frac{1}{4}\left[\overline{x}^{(1)} + \alpha^{11}\,\overline{x}^{(2)} + \alpha^{22}\overline{x}^{(3)} + \alpha^{33}\,\overline{x}^{(4)}\right] \\
\overline{x}_9 &= x_0^{(3)} + x_0^{(4)} + j(x_0^{(1)} + x_0^{(2)})
\end{aligned} \quad (5)$$

Inverse to Eq. 4 is given below as:

$$\{1\}\begin{cases} \overline{x}^{(1)} = \overline{x}_1 + \overline{x}_5^* + \overline{x}_7 + \overline{x}_{11}^* \\ x_0^{(1)} = \overline{x}_3 \cdot 1 \end{cases};\ \{2\}\begin{cases} \overline{x}^{(2)} = \overline{x}_1\alpha^{23} + \overline{x}_5^*\alpha^5 + \overline{x}_7\alpha^{17} + \overline{x}_{11}^*\alpha^{11} \\ x_0^{(2)} = \overline{x}_3 \cdot j \end{cases}$$

$$\{3\}\begin{cases} \overline{x}^{(3)} = \overline{x}_1\alpha^{22} + \overline{x}_5^*\alpha^{10} + \\ \overline{x}_7\alpha^{10} + \overline{x}_{11}^*\alpha^{22} \\ x_0^{(3)} = \overline{x}_9 \cdot 1 \end{cases};\ \{4\}\begin{cases} \overline{x}^{(4)} = \overline{x}_1\alpha^{21} + \overline{x}_5^*\alpha^{15} + \\ \overline{x}_7\alpha^3 + \overline{x}_{11}^*\alpha^9 \\ x_0^{(4)} = \overline{x}_9 \cdot j \end{cases} \quad (6)$$

The symbols "*" and "·" denote the complex conjugate and scalar (dot) product, respectively.

III. FIVE-LEVEL MODULATION ALGORITHM FOR QUAD-INVERTER TWELVE-PHASE CONVERTER

The total power, P, of the twelve-phase inverter can be expressed as the sum of the power of the four three-phase windings $P^{(1)}$ {1}, $P^{(2)}$ {2}, $P^{(3)}$ {3}, and $P^{(4)}$ {4} shown below [3]:

$$\begin{aligned} P &= P^{(1)} + P^{(2)} + P^{(3)} + P^{(4)} \\ &= \tfrac{3}{2}\overline{v}_H^{(1)} \cdot \overline{i}^{(1)} + \tfrac{3}{2}\overline{v}_H^{(2)} \cdot \overline{i}^{(2)} + \tfrac{3}{2}\overline{v}_H^{(3)} \cdot \overline{i}^{(3)} + \tfrac{3}{2}\overline{v}_H^{(4)} \cdot \overline{i}^{(4)} \end{aligned} \quad (7)$$

If the bi-directional switches for each phase and two capacitors are neglected in Fig. 2, the result is four standard isolated two-level inverters. Now, the modulations are carried out as 2-level VSIs. Applying space vector theory, the $\overline{v}$ output voltage vector of the dual six-phase inverter can be expressed as the sum of the voltage vectors of the four three-

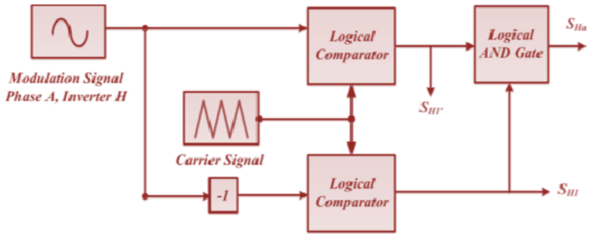

Fig. 3. Multilevel modulation scheme with one carrier for phase 'a' of inverter $VSI_H^{(1)}$.

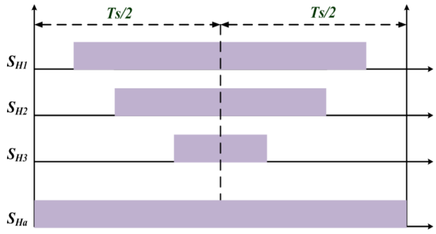

Fig. 4. PWM pattern of inverters, modulation Index = 0.8).

phase windings $\{1\}$-$\overline{v}^{(1)}$, $\{2\}$-$\overline{v}^{(2)}$, $\{3\}$-$\overline{v}^{(3)}$, and $\{4\}$-$\overline{v}^{(4)}$ of the four isolated inverters ($VSI_H^{(1)}$, $VSI_H^{(2)}$, $VSI_H^{(3)}$, $VSI_H^{(4)}$) as given below [3, 7]:

$$\overline{v} = \overline{v}_H^{(1)} + \overline{v}_H^{(2)} + \overline{v}_H^{(3)} + \overline{v}_H^{(4)} \tag{8}$$

Furthermore, by splitting twelve-phase windings into four three-phase windings as in Fig. 1,as well as considering (8) and (4), the modulating vectors can be represented for {1}, {2}, {3} and {4} three-phase windings inverters $VSI_H^{(1)}$, $VSI_H^{(2)}$, $VSI_H^{(3)}$, and $VSI_H^{(4)}$ by:

$$\overline{v}_H^{(1)} = \tfrac{1}{3}V_{DC}\left(S_{H1} + S_{H2}e^{j2\pi/3} + S_{H3}e^{j4\pi/3}\right) \tag{9}$$

$$\overline{v}_H^{(2)} = \tfrac{1}{3}V_{DC}\left(S_{H4}\alpha + S_{H5}\alpha e^{j2\pi/3} + S_{H6}\alpha e^{j4\pi/3}\right) \tag{10}$$

$$\overline{v}_H^{(3)} = \tfrac{1}{3}V_{DC}\left(S_{H7}\alpha^2 + S_{H8}\alpha^2 e^{j2\pi/3} + S_{H9}\alpha^2 e^{j4\pi/3}\right) \tag{11}$$

$$\overline{v}_H^{(4)} = \tfrac{1}{3}V_{DC}\left(S_{H10}\alpha^3 + S_{H11}\alpha^3 e^{j2\pi/3} + S_{H12}\alpha^2 e^{j4\pi/3}\right) \tag{12}$$

Now, by considering (8)-(12), the modulating vector of the symmetrical/asymmetrical twelve-phase windings can be determined for isolated or non-isolated cases. Where again, $\alpha = exp\ (j2\pi/12)$ for the symmetrical case, and $\alpha = exp\ (j\pi/12)$ for the asymmetrical case, as the displacement between inverters. Consider the switching state for the first three-phase winding inverter $VSI_H^{(1)}$, with upper-states legs $\{S_H, S_{H1}, S_{H2}, S_{H3}\}$, and lower-states legs $\{S_L, S_{L1}, S_{L2}, S_{L3}\} = \{1, 0\}$. Suppose, then that zero-sequence currents are zero, therefore resulting in balanced operation. Then (12) can be written as four separate three-phase VSIs, namely (8)-(12). To simplify the investigation and allow for clear physical meaning, the converter is triggered with a single carrier based 5-level modulation signal [15-16]. The modulating reference signals are exposed to the standard triangular carrier to maximize utilization of the DC buses and to generate multilevel outputs matching those in classical MLIs. Fig. 3 elaborates, on the single carrier (MSCFM) modulation algorithm for $VSI_H^{(1)}$, which generates the 5-level output of the leg-phase 'a'. This strategy is applied identically to all other leg-phases (b, c, d, e, f, g, h, I, j, k, l) of VSIs ($VSI_H^{(2)}$, $VSI_H^{(3)}$, $VSI_H^{(4)}$), with the appropriate phase-shifts between reference modulating signals ($\alpha = exp\ (j2\pi/12)$ symmetrical or $\alpha = exp\ (j\pi/12)$ asymmetrical) to maintain proper operation. For phase 'a', switch S_{Ha} is modulated throughout the fundamental period, that is swapped {1, 0} with the switching cycle. Switch S_{HI} is modulated by being in the ON state for half of the fundamental period (first-half) and is in the OFF state for the second half. To obtain 5-levels in all other phases (b, c, d, e, f, g, h, i, j, k, l) the same strategy is applied. Fig. 3 depicts the switch pattern for inverters $VSI_H^{(1)}$ with a modulation index of 0.8.

IV. NUMERICAL SIMULATION RESULTS AND DISCUSSION

TABLE I. MAIN PARAMETERS OF DUAL SIX-PHASE MULTILEVEL VSIS.

DC Bus	V_{DC}	= 400Volts
Load Resistances	R	= 8 Ω
Load Inductances	L	= 10mH
Fundamental Frequency	F	= 50Hz
Switching Frequency	F_S	= 5 KHz
Capacitors	V_C	= 2200μF

The effectiveness of the complete AC drive system is verified by a numerically developed model using Matlab/PLECS simulation software. Parameters are shown in Table I for investigations under balanced conditions. The modulation index of $VSI_H^{(1)}$, $VSI_H^{(2)}$, $VSI_H^{(3)}$, $VSI_H^{(4)}$ are set to 0.8 and hence overall modulation index of dual six-phase converter is 0.8. The complete, predicted behavior of the proposed symmetrical/asymmetrical dual six-phase converter system is described by Fig. 4 and Fig. 5. Fig. 4(A), Fig. 4(B), Fig. 5(C) and Fig. 5(D), are the generated line-line voltages of the first-{1}, second-{2}, third-{3}, and fourth-{4} three-phase windings VSIs ($VSI_H^{(1)}$, $VSI_H^{(2)}$, $VSI_H^{(3)}$, and $VSI_H^{(4)}$) of the symmetrical twelve-phase isolated/non-isolated converter. Additionally, these are depicted with their fundamental components and are shown to be equal in amplitude correspondingly to balanced operation. It was confirmed that line-line voltages of the four three-phase windings are spatially shifted by 30^0 as predicted. Further, each VSI is modulated to 5-levels of the developed modified, single carrier, five-level modulation (MSCFM) algorithm. Fig. 4(E), Fig. 4(F), Fig. 5(G) and Fig. 5(H), depicts the generated phase voltage of the first- (phase 'a') {1}, second- (phase 'd') {2}, third- (phase 'g') {3}, and fourth- (phase 'j') {4}, three-phase windings VSIs ($VSI_H^{(1)}$, $VSI_H^{(2)}$, $VSI_H^{(3)}$, and $VSI_H^{(4)}$). These are also depicted with their fundamental components and are shown to be equal in amplitude corresponding to balanced operation. As predicted, the voltage generated demonstrates 7-levels in all star-windings {1}, {2}, {3} and {4}. The obtained fundamental amplitude is in agreement with (8), (9), (10) and (11). Secondly, the fundamental components confirm that the phase voltages are spatial shifted by 30^0 displacements which is observed between voltages of star-windings {1} to {4}. This result was predicted by the analysis of the system. Hence smooth propagation is ensured with isolated/non-isolated dual six-phase symmetrical converter with modulation index=0.8.

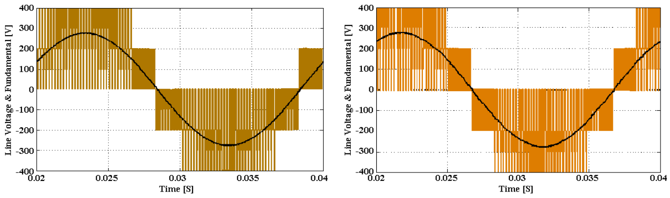

(A). Line–line voltage of inverter $\mathbf{VSI_H^{(1)}}$.

(B). Line–line voltage of inverter $\mathbf{VSI_H^{(2)}}$.

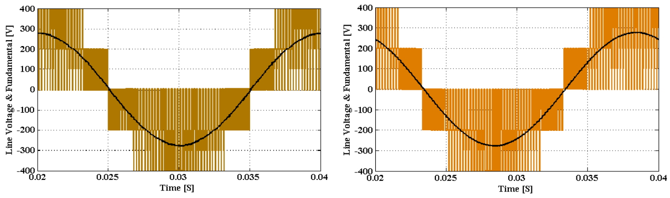

(C). Line–line voltage of inverter $\mathbf{VSI_H^{(3)}}$.

(D). Line–line voltage of inverter $\mathbf{VSI_H^{(4)}}$.

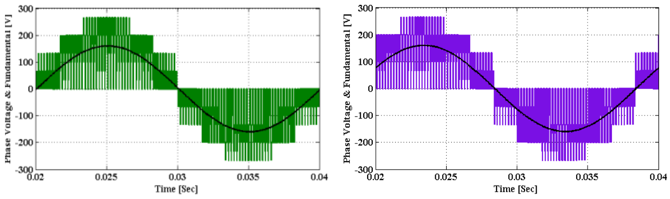

(E). First-phase voltage across the open-winding of first three-phase winding {1}.

(F). First-phase voltage across the open-winding of second three-phase winding {2}.

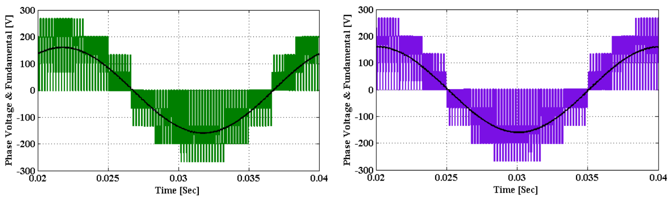

(G). First-phase voltage across the open-winding of third three-phase winding {3}.

(H). First-phase voltage across the open-winding of fourth three-phase winding {4}.

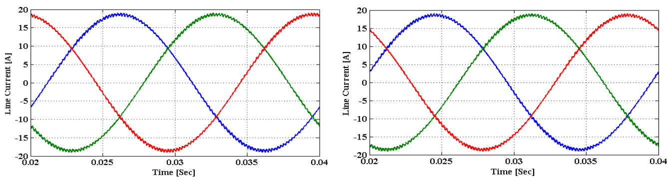

(I). First three-phase currents of the open-windings {1}.

(J). Second three-phase currents of the open-windings {2}.

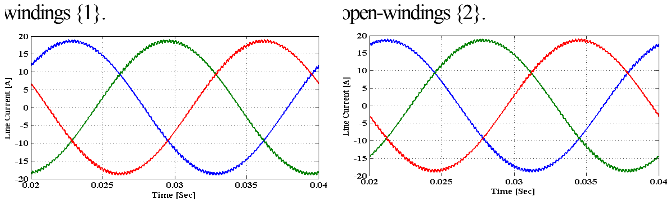

(K). Third three-phase currents of the open-windings {3}.

(L). Fourth three-phase currents of the open-windings {3}.

Fig. 4. The numerical simulation test behavior of the proposed symmetrical ($\alpha = exp\ (j2\pi/12)$) quad-inverter isolated/non-isolated dual six-phase multilevel star-winding converter. Modulation index = 0.8, kept for balanced operation. Voltages are depicted with its corresponding time averaged fundamental components.

Correspondingly, First-{1}, second-{2}, third-{3} and fourth-{4}, three-phase star-windings currents are shown in Fig. 4(I), Fig. 4(J), Fig. 4(K) and Fig. 4(L) respectively.

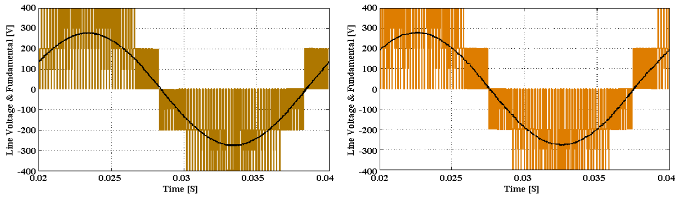

(A). Line–line voltage of inverter $\mathbf{VSI_H^{(1)}}$.

(B). Line–line voltage of inverter $\mathbf{VSI_H^{(2)}}$.

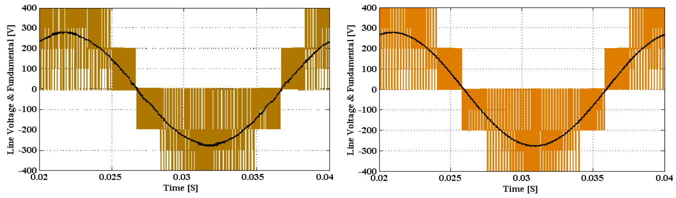

(C). Line–line voltage of inverter $\mathbf{VSI_H^{(3)}}$.

(D). Line–line voltage of inverter $\mathbf{VSI_H^{(4)}}$.

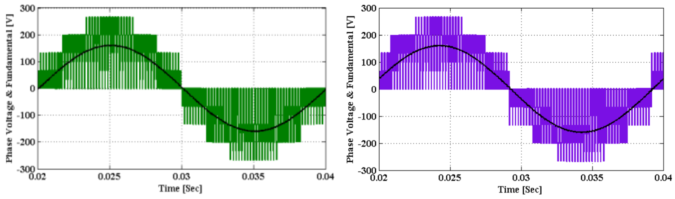

(E). First-phase voltage across the open-winding of first three-phase winding {1}.

(F). First-phase voltage across the open-winding of second three-phase winding {2}.

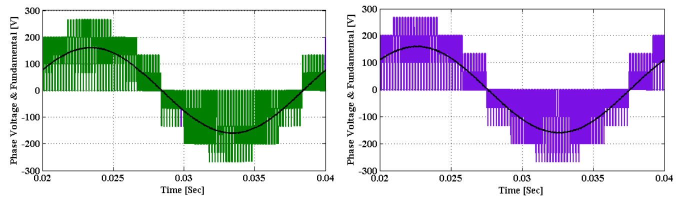

(G). First-phase voltage across the open-winding of third three-phase winding {3}.

(H). First-phase voltage across the open-winding of fourth three-phase winding {4}.

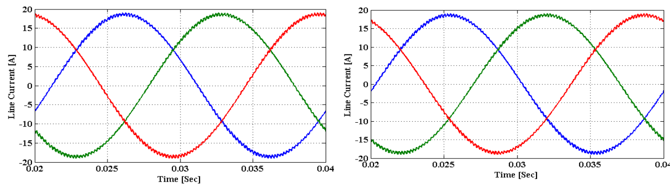

(I). First three-phase currents of the open-windings {1}.

(J). Second three-phase currents of the open-windings {2}.

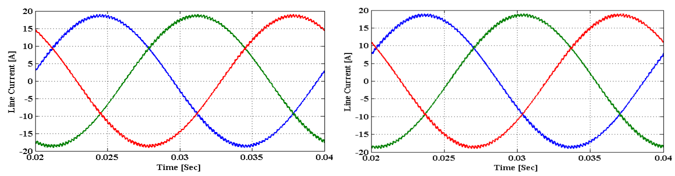

(K). Third three-phase currents of the open-windings {3}.

(L). Fourth three-phase currents of the open-windings {3}.

Fig. 5. The numerical simulation test behavior of the proposed asymmetrical ($\alpha = exp\ (j\pi/12)$) quad-inverter isolated/non-isolated dual six-phase multilevel star-winding converter. Modulation index = 0.8, kept for balanced operation. Voltages are depicted with its corresponding time averaged fundamental components.

Twelve-phase currents are sinusoidal in nature, balanced, equal in amplitude, and phase shifted by 30^0 displacements between star-windings, and smoothly propagated. Fig. 5(A),

Fig. 5(B), Fig. 5(C) and Fig. 5(D), are the generated line-line voltages of the first-{1}, second-{2}, third-{3} and fourth-{4} three-phase windings by VSIs ($VSI_H^{(1)}$, $VSI_H^{(2)}$, $VSI_H^{(3)}$, and $VSI_H^{(4)}$) of the asymmetrical twelve- phase isolated/non-isolated converter. Likewise, the fundamental components are equal in amplitude, consistent with balanced operation. It was confirmed that line-line voltages of the four three-phase windings are spatially shifted by 15^0 as predicted. Furthermore, in this case, each VSI is modulated to 5-levels of the developed modified, single carrier, five-level modulation (MSCFM) algorithm Similarly, Fig. 5(E), Fig. 5(F), Fig. 5(G) and Fig. 5(H), depicts the generated phase voltage of the first- (phase 'a') {1}, second- (phase 'd') {2}, third- (phase 'g') {3}, and fourth- (phase 'j') {4}, three-phase windings VSIs ($VSI_H^{(1)}$, $VSI_H^{(2)}$, $VSI_H^{(3)}$, and $VSI_H^{(4)}$). Again, the fundamental components are equal in amplitude, consistent with balanced operation. Firstly, as predicted, the voltages generated demonstrate 7-levels in all star-windings {1}, {2}, {3} and {4}. The obtained fundamental amplitude is in agreement with the expressions seen in (8)-(11). Secondly, the fundamental components confirm that the phase voltages are spatial shifted by 15^0 displacements which is observed between voltages of star-windings {1}, {2}, {3} and {4} which matches the prediction. Hence, smooth propagation is ensured with isolated/non-isolated dual six-phase asymmetrical converter with modulation index=0.8. Correspondingly, First-{1}, second-{2}, third-{3} and fourth-{4}, three-phase star-windings currents are shown in Fig. 5(I), Fig. 5(J), Fig. 5(K) and Fig. 5(L) respectively. As in the symmetrical case, the asymmetrical converter demonstrates twelve-phase currents that are sinusoidal in nature, balanced with equal amplitudes, phase shifts of 30^0 displacements observed between star-windings, and smoothly propagated. Hence, the depicted results prove the set theoretical expectations for isolated/non-isolated dual six-phase symmetrical converter with modulation index=0.8 with good agreement. Finally, the results confirm that the drawbacks inherent to employing a classical dual inverter configuration are overcome with the proposed topology with respect to the multilevel operation with star-windings [2, 4-7, 13-14].

V. Conclusion

An isolated/non-isolated quad-inverter configuration for a twelve-phase symmetrical/asymmetrical star-winding converter was elucidated by the work presented in this paper. Furthermore, the developed MSCFM PWM algorithm modulates each VSI as equivalent to a 5 output level, multilevel inverter. The numerical simulation software's modeling results are presented and discussed, showing balanced power operation. Therefore, the proposed twelve-phase star-winding converter overcomes the drawback of classical dual open-winding multilevel inverter configuration when applied to multiphase AC drives. Proposed dual six-phase star-winding converters can be utilized for multiple batteries (isolated version) or fuel-cell fed systems for (low-voltage/high-current) electrical vehicles, AC tractions, and 'More-Electric Aircraft' (MEA) applications. Investigations are ongoing to develop a framework to properly optimize a multilevel (5-level) converter based on the carrier-based or space vector modulation PWM generation techniques. This will be reported in future works.

References

[1] E.Levi, R.Bojoi, F.Profumo, H.AToliyat, S. Williamson, "Multi¬ phase induction motor drives – a technology status review," *IET Electr. Power Appl.,* vol. 1, no.4, pp. 489-516, July 2007.

[2] P.Sanjeevikumar, G.Grandi, Frede Blaabjerg, Patrick W. Wheeler, Olorunfemi Ojo, "Analysis and Implementation of Power Management and Control Strategy for Six-Phase Multilevel AC Drive System in Fault Condition", *Engg. Science and Tech; An Intl. J. (JESTECH), Elsevier Pub.,* 13 Jul. 2015. Doi: 10.1016/j.jestch. 2015.07.007.

[3] R.Bojoi, F.Farina, F.Profumo, A.Tenconi, "Dual three-phase induction machine drives control— A survey," *IEE J. Trans. on Ind. Appl.,* vol. 126, no. 4, 2006.

[4] G. Grandi, P. Sanjeevikumar, D. Ostojic, C. Rossi, "Quad-inverter configuration for multi-phase multi-level ac motor drives", *Conf. Proc., Intl. Conf. Computational Technologies in Elect. and Electron. Engg., IEEE–SIBIRCON'10,* Irkutsk Listvyanka (Russia), pp. 631–638, 11–15 Jul. 2010.

[5] P.Sanjeevikumar, G.Grandi, Frede Blaabjerg, Joseph Olorunfemi Ojo, Patrick W.Wheeler, "Power Sharing Algorithm for Vector Controlled Six-Phase AC Motor with Four Customary Three-Phase Voltage Source Inverter Drive", *Engg. Science and Tech; An Intl. J. (JESTECH), Elsevier Pub.,* vol. 16, no. 3, pp. 405–415, 11 Feb. 2015.

[6] G. Grandi, P. Sanjeevikumar, Y. Gritli, F. Filippetti, "Experimental investigation of fault-tolerant control strategies for quad-inverter converters", *Conf. Proc. IEEE Intl. Conf. on Electrical System for Aircraft, Railway and Ship Propulsion, IEEE-ESARS'12*, Bologna (Italy), pp. 1-8, 16–18 Oct. 2012.

[7] A.Tani, M.Mengoni, L. Zarri, G.Serra, D.Casadei, "Control of multi-phase induction motors with an odd number of phases under open circuit faults", *IEEE Trans. on Power Electronics,* vol. 27, no. 2, pp. 565-577, 2012.

[8] W. Cao, B.C. Mecrow, G.J. Atkinson, J.W. Bennett, D.J. Atkinson, "Overview of electric motor technologies used for More-Electric Aircraft (MEA)", *IEEE Trans. on Ind. Electron*., vol. 59, no. 9, pp. 3523-3531, Sept. 2012.

[9] F. Scuiller, J.F. Charpentier, E. Semail, "Multi-star multi-phase winding for a high power naval propulsion machine with low ripple torques and high fault tolerant ability," *Proc. of Vehicle Power and Propulsion Conference,* Lille, France, pp. 1-5, 1-3 Sept. 2010.

[10] L. G. Franquelo, J. Rodriguez, J. I. Leon, S. Kouro, R. Portillo and M. M. Prats, "The age of multilevel converters arrives," *IEEE Ind. Electron. Magazine*, vol. 2, no. 2, pp. 28–39, June 2008.

[11] Frede Blaabjerg, M.M.Pecht, "Robust Design and Reliability of Power Electronics", *IEEE Trans. on Power Electron.,* vol. 30, no. 5, pp. 2373-2374, 2015.

[12] S. Yang, A. Bryant, P. Mawby, D. Xiang, Li Ran, P. Tavner, "An industry-based survey of reliability in power electronic converters," *IEEE Trans. on Ind. Electron.,* vol. 47, no. 3, pp. 1441–1451, May–June 2011.

[13] Feng Gao, P.Chiang Loh, F.Blaabjerg,"Dual Z-Source Inverter With Three-Level Reduced Common-Mode Switching", *IEEE Trans. on Ind. Appl.,* vol. 43, no. 6, pp. 1597-1608, Nov. 2007.

[14] S.Chowdhury, Patrick Wheeler, Chris Gerada, S. Lopez Arevalo, "A dual inverter for an open end winding induction motor drive without an isolation transformer", *Conf. Proc. IEEE Applied Power Electronics Conference and Exposition, IEEE-APEC'15*, Charlotte, NC, USA, pp. 283-289, 15-19 March 2015.

[15] P.Sanjeevikumar, Frede Blaabjerg, Patrick Wheeler, Olorunfemi Ojo, "Three-phase multilevel inverter configuration for open-winding high power application", *Conf. Proc., The 6th IEEE Intl. Symp. on Power Electron. for Distributed Generation Systems, IEEE-PEDG'15,* Aachen (Germany), 22–25 June 2015.

[16] P.Sanjeevikumar, Frede Blaabjerg, Patrick Wheeler, Olorunfemi Ojo, Kiran P. Maroti, "A Novel Double Quad-Inverter Configuration for Multilevel Twelve-Phase Open- Winding Converter", *Conf. Proc. of 7th IEEE Intl. Conf. on Power System, IEEE-ICPS'16,* Indian Institute of Technology (IIT-Delhi), Delhi (India), 4–6 Mar. 2016.